

A Novel Spectral/Temporal Encryption Block for Multiple Access OCDMA Network Adopting Spectral Flexible Weight Code

Mohamed RAHMANI¹, Ghoutia Naima SABRI², Abdelhamid CHERIFI³

¹The Information and Telecommunications Processing Laboratory (LTIT), Electrical Engineering Department, Faculty of Technology, TAHRI Mohamed University of Bechar, Bechar, Algeria

²The Information and Telecommunications Processing Laboratory (LTIT), Department of Material Sciences, Faculty of Exact Sciences, TAHRI Mohamed University of Bechar, Bechar, Algeria

³Technology of Communication Laboratory (LTC), University of Tahar Moulay, Saida, Algeria

E-mail: rahmani.mohamed@univ-bechar.dz ; sabri.ghoutia@univ-bechar.dz

Abstract - The main tasks of optical code division multiple access (OCDMA) systems are increasing transmission capacity while minimizing phase-induced intensity noise (PIIN). In this paper, a novel two-dimensional spectral/temporal spectral flexible weight (2D-SFW) code for non-coherent spectral amplitude coding (SAC) systems is given. The code was designed to overcome the limitations of one-dimensional codes that include system complexity and multiple access interferences (MAI), as well as boost system capacity and enable a high data rate. Under the impact of capacity rate, and consumed power the proposed code (2D-SFW) outperforms existing two-dimensional codes such as Dynamic Cyclic Shift (2D-DCS), Multi-service (2D-MS), and Zero Cross Correlation/Multi-Diagonal (2D-ZCC/MD) codes in terms of bit error rate (BER) and signal-to-noise ratio (SNR). signals.

Keywords – BER, OCDMA, PIIN, SFW, SNR.

I. INTRODUCTION

Optical communications have grown in popularity in recent years due to the benefits they bring, such as the capacity to exchange information across extended distances and transport data at extremely fast speeds [1]. The majority of today's optical communication systems rely upon multiple access technologies, especially optical code division multiple access (OCDMA). Furthermore, the OCDMA system is employed for allocating each transmission block (user) a unique optical code, meaning that this method enables the simultaneous transmission of numerous users in the same transmission environment while utilizing the full frequency range at any moment [2].

Relying on the optical source, the OCDMA technique is partitioned into two systems: coherent OCDMA and incoherent OCDMA. The

first category permits the creation of absolutely orthogonal optical codes using bipolar bits (-1 and +1), which completely eliminates the problem of multiple access interferences (MAI) between users, whereas the second enables the building of non-strictly orthogonal optical codes using unipolar bits (0 and +1), leading to the MAI due to the insufficient orthogonality between codes [3]. However, by avoiding the overlapping of "1"s in the sequence of codes of several users, it is possible to develop unipolar orthogonal codes that allow the MAI to be controlled [4].

Excessive phase-induced intensity noise (PIIN) created by multi-users chips interferences leads to multi-user interference (MUI or MAI), which largely degrades the performance of the OCDMA system. Moreover, spectral amplitude coding (SAC) is a prominent coding approach in OCDMA systems for producing optical codes and avoiding MAI problems [5]. For that, several one-

dimensional (1D) codes have been designed to minimize PIIN noise and MAI effects.

To avoid these limits, one of the essential stages in determining overall system performance is a proper selection of codes with strong orthogonality. This technical term (orthogonality) is known as the zero cross-correlation (ZCC) property.

Nevertheless, an increasing number of users in one-dimensional 1D-OCDMA systems necessitate a large number of codes, which means longer spectral lengths; at this point, lengthy code length necessitates high power consumption, which becomes the primary factor degrading the performance of 1D-OCDMA systems [6]. To overcome these challenges, the researchers focused their research on the development of one-dimensional (1D) codes for the two-dimensional (2D) domain for the purpose of lowering the length and increasing the number of concurrent users [7].

The two-dimensional codes can be developed by combining two axes (spectral, spatial, temporal, and polarization), hence, the most typical approaches for two-dimensional OCDMA systems are spectral/time and spectral/spatial schemes. In this context, various 2D codes have been developed, In [8], the two-dimensional Extended Enhanced Double Weight (2-D Extended-EDW) code has been studied to improve the system's performance of OCDMA. In [9], a two-dimensional enhanced multi-diagonal (2D-EMD) code is employed to enhance the optical CDMA system. In [10], two-dimensional multi-service (2D-MS) code has been suggested in order to overcome MAI effects and increase system capacity. In [11], the two-dimensional Diagonal Eigenvalue Unity (2D-DEU) code is proposed to reduce the MAI. In [12], the two-dimensional spectral/spatial dynamic cyclic shift (2D-DCS) code also has been investigated. [13], investigates a two-dimensional hybrid flexible cross-correlation (FCC)/modified double weight (MDW) code for the spectral/time OCDMA system, where the first component is assigned by FCC code and the second axis is assigned by MDW code.

The setup of a spectral/spatial scheme typically involves the use of numerous optical fibers (spatial encoding) between the sending and receiving ends, increasing the system's complexity and expense. Using temporal encoding, on the other hand, is more appropriate for avoiding employing multiple spatial components. For OCDMA networks given by wavelength/time spreading, 2D-spectral/temporal (S/T) codes are deemed effective, where the pulses are set in separate chips over the bit period and each chip has a different wavelength.

In this respect, the current study introduces a new two-dimensional spectral flexible weight (2D-SFW) code for spectral/temporal OCDMA with high multiplexing capacity and simplicity of construction, enabling a system that consumes less power due to direct spectral detection at the receiver. In addition, the recommended code has a zero-correlation property (ZCC), which excludes MAI effects and diminishes PIIN noise. By overcoming PIIN and reducing MAI, the system capacity is increased by taking into consideration the impacts of PIIN, shot noise, and thermal noise at the receiver level (photodetector). The findings from the analysis show that the proposed code outperforms the codes discussed in [10,12,14].

The rest of this work is organized as follows: the second section details the construction of a new two-dimensional spectral/temporal 2D-SFW code, the third section presents a 2D-SFW OCDMA architecture, the fourth section provides a mathematical analysis in terms of SNR, BER, and error vector magnitude (EVM) expressions, the fifth section presents and discusses the results obtained of our system. Finally, the conclusion relating to the effectiveness of our model is stated in the sixth section.

II. DESIGN OF A SPECTRAL FLEXIBLE WEIGHT CODE

A) *One Dimensional Code*

The spectral flexible weight (SFW) code is created by combining three parameters (L, W, K), where "L" represents the spectral length of each sequence, "W" represents the number of "1" in each sequence (code weight), and "K" represents

the number of users (number of codes). Hence, the stages of its construction are listed below:

1. Choose the number of users and the code weight (K, W).
2. Generate two matrices: even weight diagonal matrix (EWDM) and odd weight anti diagonal matrix (OWAM), where EWDM and OWAM are presented as follows:

$$EWDM = \begin{bmatrix} \overbrace{1 \dots 1}^{W \text{ even}} & 0 & 0 \\ 0 & 1 \dots 1 & \vdots \\ \vdots & \vdots & 0 \\ 0 & 0 & 1 \dots 1 \end{bmatrix}_{K \times WK} \quad (1)$$

$$OWAM = \begin{bmatrix} c_1 & c_i & c_K \\ \tilde{0} & \tilde{0} & \tilde{1} \\ 0 & \cdot & 0 \\ \underbrace{1}_{W \text{ odd}} & 0 & 0 \end{bmatrix}_{K \times K} \quad i = 1, 2, \dots, K \quad (2)$$

3. When the weight is odd, perform the superposition of the two matrices as follows:

$$SFW_{W(odd)} = \begin{bmatrix} c_1 & c_2 & c_K \\ 1 & \tilde{0} & 1 & 0 & \tilde{0} & 0 & \dots & \tilde{1} & 0 \\ 0 & \vdots & 0 & 1 & \vdots & 1 & \dots & 0 & \vdots \\ \vdots & \vdots & 0 & 0 & 0 & 0 & \dots & \vdots & \vdots \\ \vdots & 0 & \vdots & \vdots & 1 & \vdots & \dots & \vdots & 0 \\ 0 & 1 & 0 & 0 & 0 & 0 & \dots & 0 & 1 \end{bmatrix} \quad (3)$$

4. When the weight is even, only EWDM is used as follows:

$$SFW_{W(Even)} = \begin{bmatrix} \overbrace{1 \dots 1}^W & 0 & 0 \\ 0 & 1 \dots 1 & \vdots \\ \vdots & \vdots & 0 \\ 0 & 0 & 1 \dots 1 \end{bmatrix}_{K \times WK} \quad (4)$$

5. Using the following formulae, determine the length of the SFW code and its auto/cross correlation property:

$$\begin{cases} L = K \times W \\ \sum_{i=1}^K C_i C_j = \begin{cases} \lambda_a = W & \text{if } i = j \\ \lambda_c = 0 & \text{if } i \neq j \end{cases} \end{cases} \quad (5)$$

Here λ_a and λ_c are auto-correlation and cross-correlation, respectively. C_i, C_j are two sequences of SFW code. Table I gives an example of a one-dimensional SFW code (1D-SFW) for $K=3$ and $W=2$ and 3 , respectively.

Table I. 1D-SFW spectral code for 3 users

	Even weight (K=3, W=2)
1D-SFW code	$\begin{bmatrix} 1 & 1 & 0 & 0 & 0 & 0 \\ 0 & 0 & 1 & 1 & 0 & 0 \\ 0 & 0 & 0 & 0 & 1 & 1 \end{bmatrix}$
	Odd weight (K=3, W=3)
1D-SFW code	$\begin{bmatrix} 1 & 0 & 1 & 0 & 0 & 0 & 0 & 1 & 0 \\ 0 & 0 & 0 & 1 & 1 & 1 & 0 & 0 & 0 \\ 0 & 1 & 0 & 0 & 0 & 0 & 1 & 0 & 1 \end{bmatrix}$

B) Two-Dimensional S/T Code

The 2D-SFW code is derived from the 1D-SFW code and can be built by combining spectral sequence (X) and temporal sequence (Y), respectively. Let X_g represent $[x_0, x_1, \dots, x_{l_1-1}]$ and Y_h represent $[y_0, y_1, \dots, y_{l_2-1}]$ be two 1D-SFW sequences. P_1 and P_2 are their code weights. $l_1 = P_1 \times C_1$ is the spectral length, and $l_2 = P_2 \times C_2$ is the temporal length, where C_1 and C_2 are the X and Y cardinalities.

The design of 2D-SFW can be stated as follows [15]:

$$A_{g,h} = Y_h^T X_g \quad (6)$$

Furthermore, in order to eliminate the influence of MAI in 2D-SFW, we define four characteristic matrices $A^{(d)}$, where $d \in (0, 1, \dots, 3)$ [16]:

$$\begin{cases} A^{(0)} = Y^T X \\ A^{(1)} = Y^T \bar{X} \\ A^{(2)} = \bar{Y}^T X \\ A^{(3)} = \bar{Y}^T \bar{X} \end{cases} \quad (7)$$

Table II displays the proposed code sequence designated by $A_{g,h}$ in (7). Table III explains the new 2D-SFW code's cross-correlation property, which is as follows:

$$\begin{aligned} R^{(d)}(g, h) &= \sum_{i=0}^{l_1-1} \sum_{j=0}^{l_2-1} a_{i,j}^{(d)} a_{(i+g)(j+h)} \\ &= \begin{cases} P_1 P_2 & \text{when } g = 0 \cap h = 0 \\ 0 & \text{else} \end{cases} \end{aligned} \quad (8)$$

The developed 2D-SFW code's cardinality and its length are represented as follows:

$$\begin{cases} C = C_1 \times C_2 \\ L = l_1 \times l_2 \end{cases} \quad (9)$$

A 3D graphical representation of our 2D-SFW code of the first sequence is given in Fig.1

TABLE 2. 2D-SFW CODE FOR ($P_1 = C_1 = P_2 = C_2 = 2$)

	$X_0 =$	$X_1 =$
	[1 1 0 0]	[0 0 1 1]
$Y_0^T = \begin{bmatrix} 1 \\ 1 \\ 0 \\ 0 \end{bmatrix}$	$\begin{bmatrix} 1 & 1 & 0 & 0 \\ 1 & 1 & 0 & 0 \\ 0 & 0 & 0 & 0 \\ 0 & 0 & 0 & 0 \end{bmatrix}$	$\begin{bmatrix} 0 & 0 & 1 & 1 \\ 0 & 0 & 1 & 1 \\ 0 & 0 & 0 & 0 \\ 0 & 0 & 0 & 0 \end{bmatrix}$
$Y_1^T = \begin{bmatrix} 0 \\ 0 \\ 1 \\ 1 \end{bmatrix}$	$\begin{bmatrix} 0 & 0 & 0 & 0 \\ 0 & 0 & 0 & 0 \\ 1 & 1 & 0 & 0 \\ 1 & 1 & 0 & 0 \end{bmatrix}$	$\begin{bmatrix} 0 & 0 & 0 & 0 \\ 0 & 0 & 0 & 0 \\ 1 & 1 & 1 & 1 \\ 1 & 1 & 1 & 1 \end{bmatrix}$

TABLE 3. CROSS CORRELATION VALUE OF S/T 2D-SFW CODE.

	$R^{(0)}(g, h)$	$R^{(1)}(g, h)$	$R^{(2)}(g, h)$	$R^{(3)}(g, h)$
$g = 0 \cap h = 0$	$P_1 P_2$	0	0	0
$g = 0 \cap h \neq 0$	0	$P_1 P_2$	0	0
$g \neq 0 \cap h = 0$	0	0	$P_1 P_2$	0
$g \neq 0 \cap h \neq 0$	0	0	0	$P_1 P_2$

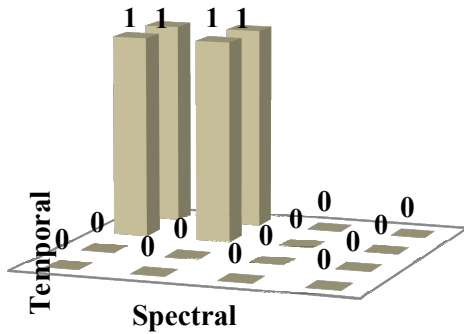


Fig. 1. 3D graphical representation of our 2D-SFW code of the first sequence of Table II.

III. 2D-SFW-OCDMA MODEL

The schematic architecture of the planned spectral/Temporal OCDMA model that employs SFW code through an optical channel is depicted in Fig. 2. The electrical signal of each user is modulated and converted into an optical signal thanks to an external modulator MZM (Mach-Zehnder modulator) using an optical source. Secondly, the resulting optical signals are sent to

a two-dimensional OCDMA encoder to implement the spectral/Temporal coding, wherein in the first phase the optical signals are connected with a W-FBGs type spectral coder (fiber Bragg grating) according to the spectral sequence of SFW code to form the one-dimensional spectral coding, then the symmetrically encoded pulses are submitted to delay lines to implement temporal coding in accord to the SFW temporal sequence as clarified in Fig. (2.a), in this point, the data is spectrally/temporally encoded according to the optical SFW code respectively. Finally, the optical signals of all users are multiplexed into a composite optical signal and sent to the optical channel.

In the receiver part, the inverse operations of the transmitter are applied as shown in Fig. (2.b). In addition, the receiver principle is divided into two steps. Firstly, the arrived pulse is coupled by a temporal decoder (delay lines) for decoding by following the temporal SFW code sequence, then the temporally decoded pulses are attached by FBGs to implement spectral decoding by following the spectral SFW code sequence, in this case, the pulses are decoded temporally/spectrally respectively. Secondly, the resulting pulses are directly spotted by a single photo-detector (PD) due to the ZCC property of our code and converted into the electrical domain, thereafter, the resulting electrical signal is filtered by a low pass Bessel filter (LPBF) to recover the original information and eliminate unwanted signals.

IV. MATHEMATICAL ANALYSIS

Some hypotheses are presented in order to facilitate the analysis of the S/T-SFW-OCDMA system: Firstly, the spectral spread of an unpolarized optical source is flat and broadband over the interval $[v_0 - \Delta v/2, v_0 + \Delta v/2]$, where v_0 is the central frequency and Δv is the light source's bandwidth. Second, all of the data sent by each user to the receivers comes at the same time. Third and fourth, the power and spectrum width of each transmitter's spectral components are identical [17].

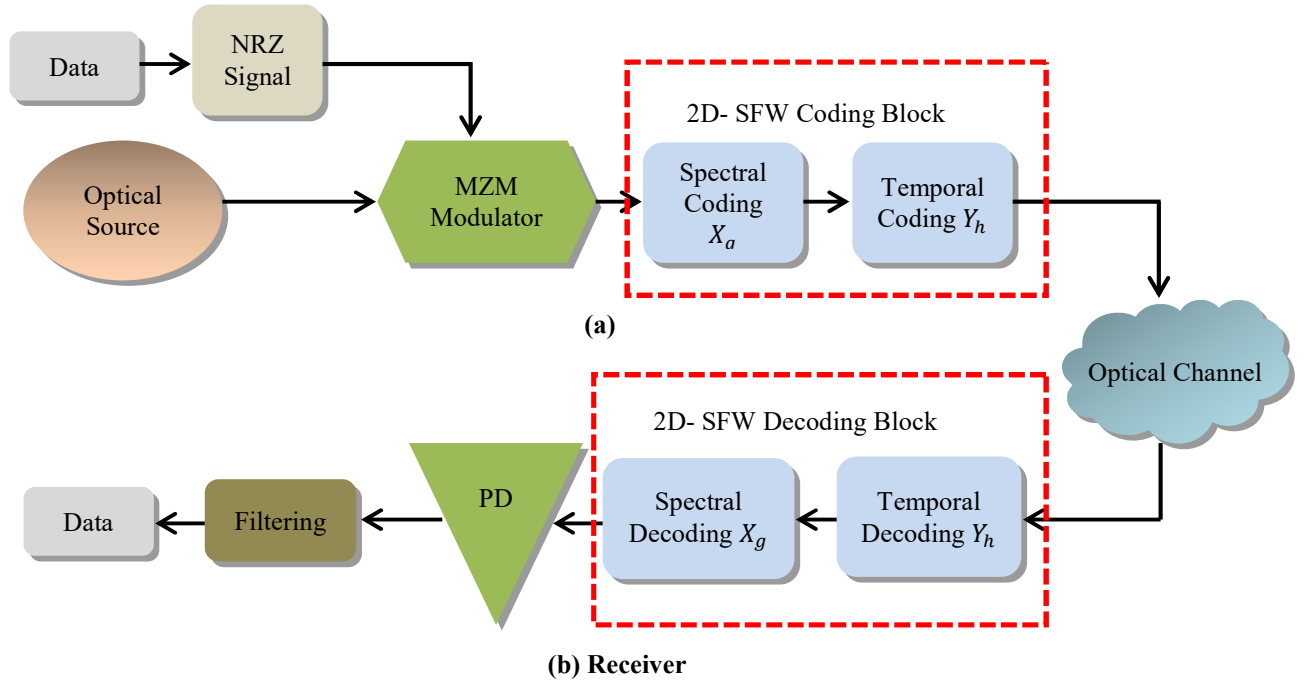


Fig. 2. Schematic architecture of the spectral/spatial OCDMA model.

Overall, two main criteria are used to evaluate the performance of an optical system: BER, which is defined as the ratio of erroneous bits to transmitted bits, and SNR, which is the ratio of received power to total noise power that affects the system. Furthermore, thanks to the ZCC feature of the S/T-SFW code, user overlaps in the optical spectrum are completely ignored, removing the effect of MAI. Thermal noise, shot noise, and PIIN noise are all discussed in this context. As a result, the SNR and total variance noise from the photo-detector are stated as follows [18]:

$$SNR = \frac{I^2}{\langle i_{noise}^2 \rangle} \quad (10)$$

$$\langle i_{noise}^2 \rangle = \langle i_{Th}^2 \rangle + \langle i_{Sh}^2 \rangle + \langle i_{PIIN}^2 \rangle \quad (11)$$

Following the aforementioned hypotheses, the power spectral density (PSD) of the received signal is written as follows [19]:

$$r(v) = \frac{P_{Sr}}{P_2 \Delta v} \sum_{w=1}^C d(W) \sum_{i=0}^{l_1-1} \sum_{j=0}^{l_2-1} a_{i,j}^{(0)} a_{i,j}(w) \Pi(v, i) \quad (12)$$

P_{Sr} , Δv , and $\Pi(v, i)$ are the effective received power, optical bandwidth, and the i^{th} spectral element of the broadband source (BBS) respectively. Where $\Pi(v, i)$ is defined as [20]:

$$\Pi(v, i) = \left\{ u \left[v - v_0 - \frac{\Delta v}{2M} (-2l_1 + 2i) \right] - u \left[v - v_0 - \frac{\Delta v}{2l_1} (-Ml_1 + 2i + 2) \right] \right\} = u \left[\frac{\Delta v}{l_1} \right] \quad (13)$$

$u[v]$ is a unit step function defined as:

$$u(v) = \begin{cases} 1 & \text{whene } v \in [0, +\infty[\\ 0 & \text{whene } v \in [-\infty, 0[\end{cases} \quad (14)$$

The photocurrent delivered by the photodiode (PD) at the receiver level can be expressed as:

$$I = \int_0^{+\infty} r(v) dv = \int_0^{+\infty} \frac{\mathcal{R} P_{Sr}}{P_2 \Delta v} \sum_{w=1}^C d(W) \sum_{i=0}^{l_1-1} \sum_{j=0}^{l_2-1} a_{i,j}^{(0)} a_{i,j}(w) \Pi(v, i) dv = \frac{\mathcal{R} P_{Sr} P_1}{l_1} \quad (15)$$

\mathcal{R} is the photodiode responsivity given as $\mathcal{R} = \eta e / h \nu_0$, where η is the quantum efficiency of the photodiode, h is Plank's constant and e is the electron charge.

The phase-induced intensity noise variance (PIIN) is calculated as follows [21]:

$$I_{PIIN}^2 = B_r I^2 \tau_c \quad (16)$$

Where B_r is electrical bandwidth, τ_c is the light coherence time which is given as [6]:

$$\tau_c = \frac{\int_0^{+\infty} r^2(v) dv}{\left[\int_0^{+\infty} r(v) dv \right]^2} \quad (17)$$

$$\begin{aligned} I_{PIIN}^2 &= B_r \mathcal{R}^2 \int_0^{+\infty} r^2(v) dv \\ &= B_r \mathcal{R}^2 \int_0^{+\infty} \left[\frac{P_{sr}}{P_2 \Delta v} \sum_{w=1}^C d(W) \sum_{i=0}^{l_1-1} \sum_{j=0}^{l_2-1} a_{i,j}^{(0)} a_{i,j}(w) \Pi(v,i) \right]^2 \\ &= \frac{B_r \mathcal{R}^2 P_{sr}^2 \Delta v}{P_2^2 \Delta v^2 l_1} [(1+0) \times (P_1 P_2)]^2 \end{aligned}$$

Hence :

$$I_{PIIN}^2 = \frac{B_r \mathcal{R}^2 P_{sr}^2 P_1^2}{\Delta v l_1} \quad (18)$$

Furthermore, thermal noise and shot noise are denoted as [21]:

$$I_{th}^2 = \frac{4K_b T_n B_r}{R_L} \quad (19)$$

$$I_{sh}^2 = 2eB_r I = 2eB_r \frac{\mathcal{R} P_{sr} P_1}{l_1} \quad (20)$$

Where $I, K_b, T_n,$ and R_L are the average photocurrent, Boltzmann's constant, absolute temperature, and load resistor respectively.

Lastly, the overall noise is calculated by plugging (18), (19), and (20) into (11) as follows:

$$\langle i_{noise}^2 \rangle = \frac{4K_b T_n B_r}{R_L} + 2eB_r \frac{\mathcal{R} P_{sr} P_1}{l_1} + \frac{B_r \mathcal{R}^2 P_{sr}^2 P_1^2}{\Delta v l_1} \quad (21)$$

Since the transmission of bits "1" and "0" is equally probable, (21) becomes:

$$\langle i_{noise}^2 \rangle = \frac{4K_b T_n B_r}{R_L} + eB_r \frac{\mathcal{R} P_{sr} P_1}{l_1} + \frac{B_r \mathcal{R}^2 P_{sr}^2 P_1^2}{2\Delta v l_1} \quad (22)$$

The expression of SNR is stated as follows based on the conclusions of (15) and (22).

$$SNR = \frac{I^2}{\langle i_{noise}^2 \rangle} = \frac{\left(\frac{\mathcal{R} P_{sr} P_1}{l_1} \right)^2}{\frac{4K_b T_n B_r}{R_L} + eB_r \frac{\mathcal{R} P_{sr} P_1}{l_1} + \frac{B_r \mathcal{R}^2 P_{sr}^2 P_1^2}{2\Delta v l_1}} \quad (23)$$

Consequently, the BER is deduced from the SNR using the Gaussian approximation and is denoted as:

$$BER = \frac{1}{2} \operatorname{erfc} \sqrt{\frac{SNR}{8}} \quad (24)$$

According to the BER formula, the EVM (%) can be stated as:

$$EVM(\%) = \sqrt{\left(\frac{1}{SNR} \right)} \times 100 \quad (25)$$

V. RESULTS AND DISCUSSION

The performance of the 2D-SFW-OCDMA approach is numerically examined in this part by comparing it to the two-dimensional codes DCS, ZCC/MD, and MS given in [10, 12, 14], where all codes have the same length. Table IV also illustrates the parameters adopted in the computational calculation. The performance of our suggested code is mainly assessed using two parameters, BER and SNR, in terms of the number of active users K and data rate R_b . Thermal noise, shot noise, and PIIN noise are also considered during the numerical calculation.

Table 3. ADOPTED PARAMETERS FOR NUMERICAL CALCULATION.

Parameters	Value
Photo detector responsivity (\mathcal{R})	0.6
Data rate (R_b)	1 Gbps
Electric bandwidth (B_r)	$0.5 \times R_b$ GHz
Receiver Load resistor (R_L)	1030 Ω
Spectral width of light (Δv)	3.75 THz
Effective source power (P_{sr})	-10 dBm
Receiver noise Temperature (T_n)	300 K
Electron charge (e)	1.6×10^{-19} c
Boltzman's constant (K_b)	1.38×10^{-23} J/K

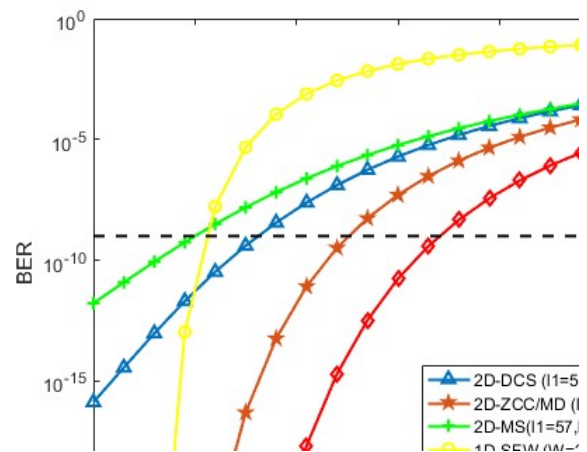


Fig. 3. BER regarding cardinality.

Figure 3 highlights the BER versus the number of subscribers when the effective source

power and bit rate are -10 dBm and 1 Gb/s, respectively, and all codes maintain the same length. At an allowable $BER = 10^{-9}$, the 2D-SFW code can reach 188 simultaneous users, whereas the 1D-SFW, 2D-DCS, 2D-MS, and 2D-ZCC/MD codes can reach 54, 83, 51, and 125 users, respectively. Thus, cardinality boosts 3.48 times of 1D-SFW, 2.26 times of 2D-DCS, 3.76 times of 2D-MS, and 1.5 times of 2D-ZCC/MD codes, respectively. The SFW code's zero cross-correlation characteristic explains this efficacy, which eliminates multiple access interference (MAI) and makes the system more appropriate for a large number of users.

Fig. 4 depicts the alteration of BER vs consumed power when the data stream is equal to 1 Gb/s and the number of available subscribers is fixed at 65. It is clear that our code requires less power than other codes. The recommended code consumes a lower power reach of -16.3 dBm at tolerable $BER = 10^{-9}$, whereas the 1D-SFW, 2D-DCS, 2D-MS, and 2D-ZCC/MD codes consume power up to -10 dBm, -11.3 dBm, -10 dBm, and -13.2 dBm, respectively. Hence, the used power from 2D-DCS can be reduced to -4.5 dBm, -6.3 dBm from 2D-MS, and -3.1 dBm from 2D-ZCC/MD codes. As a result, passing from 1D to 2D can maintain power up to -6.3 dBm.

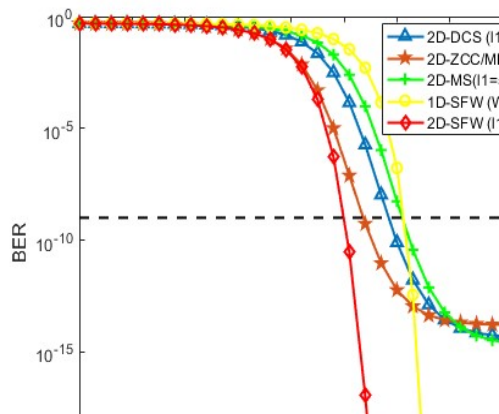


Fig. 4. BER regarding received power.

Fig. 5 depicts the BER curve as a function of spectral width when the number of active users is

set to 65, the data rate is set to 1 Gb/s, and the effective source power is set to -10 dBm. The value of BER is obviously inversely proportional to the spectral width. The suggested code 2D-SFW requires a narrow spectral width reaching 1 THz with the same code length and at an acceptable $BER = 10^{-9}$, whereas 2D-DCS, 2D-MS, and 2D-ZCC/MD codes require a bandwidth equal to 4.5 THz, 7 THz, and 2.6 THz, respectively. Consequently, our proposed approach reduces the spectrum bandwidth in comparison to 2D-DCS, 2D-MS, and 2D-ZCC/MD codes to 3.5 THz, 6 THz, and 1.6 THz, respectively.

When the number of active users is set to 65 and all codes have the same spectral/temporal length, Fig. 6 reveals the resulting PIIN noise curve from the photo-detector as a function of transmitted power variation. It is clear that the intensity of the PIIN noise grows as the system power increases. Furthermore, our 2D-SFW code has very low PIIN noise following spectral detection at the photo-detector (PD) level, whereas the 2D-DCS, 2D-MS, and 2D-ZCC/MD codes have excessively high PIIN noise when compared to the SFW code. The suggested 2D-SFW model outperforms the others in terms of reduced PIIN noise power due to ZCC's ability to significantly reduce PIIN noise.

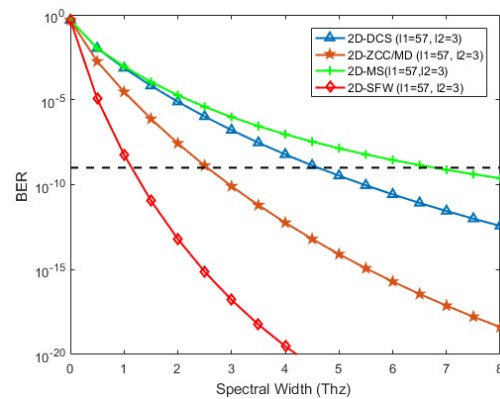


Fig. 5. BER versus spectral width.

Assuming that all codes have the same length and that the effective source power and data rate are -10 dBm and 1 Gb/s, respectively, Fig. 7

shows the EVM alteration in relation to the number of active users. Our 2D-SFW-OCDMA approach can accommodate 216 simultaneous users at a normalized EVM(%) value in the communication requirement (10%), while the 1D-SFW, 2D-DCS, 2D-ZCC/MD, and 2D-MS codes can support 75, 141, 163, and 102 active users, respectively. Thus, this advantage can be explained by the ZCC feature of the proposed SFW code, which limits MAI and boosts the system's suitability for a high capacity of users as well as its short spectral and spatial length.

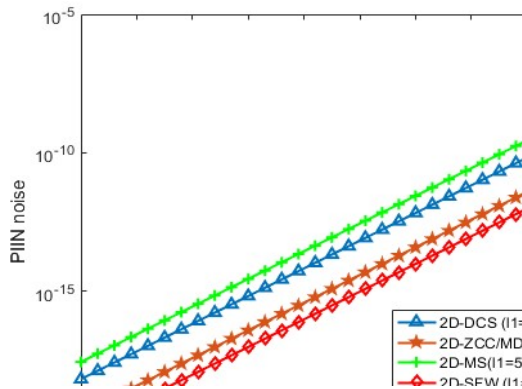


Fig. 6. PIIN noise regarding effective power.

Fig. 8 explores the alteration of BER regarding the bit rate when the consumed power is at -10 dBm and the available subscribers is fixed at 65. We can observe that the proposed 2D-SFW-OCDMA approach accommodates a higher data stream in parallel with other codes, where our code accommodates reach 4.2 Gb/s data rate, whereas 2D-DCS accommodates 1.12 Gb/s, while 2D-ZCC/MD and 2D-MS codes accommodate 2.41 Gb/s, 1.11 Gb/s respectively. Furthermore, the same code in 2D encoding can accommodate 0.79 Gb/s, thus, the proposed spectral/temporal 2D-SFW code improved the data rate by 3.75 times than the 2D-DCS code, 1.74 times than the 2D-ZCC/MD code, and 3.78 times than the 2D-MS code respectively; as well as, the transit of 1D to 2D encrypting for the same code enhance the bit rate by 5.31 times respectively.

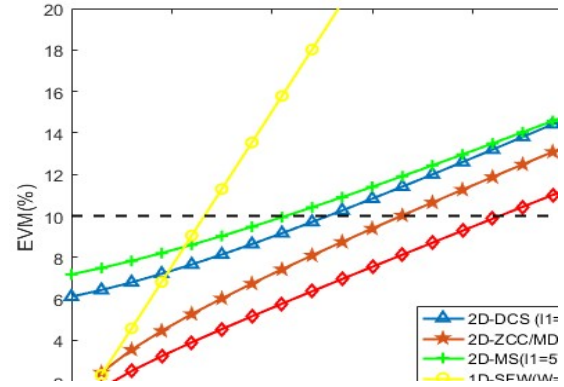


Fig. 7. EVM (%) regarding active users.

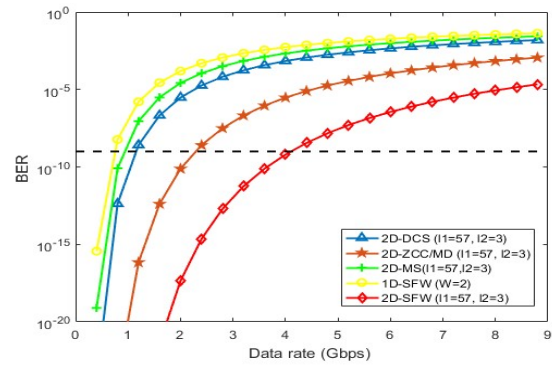


Fig. 8. BER regarding data rate.

VI. CONCLUSION

This study developed a new two-dimensional spectral/temporal (S/T) coding family for an incoherent OCDMA network. Through the application of the ZCC feature, the new designed 2D-SFW code eliminates cross-correlation between any two distinct users, minimizes phase-induced intensity noise (PIIN), and ignores entirely multiple access interferences (MAI). Each user is allocated a code word constituted of a spectral code sequence and a temporal code sequence. According to the numerical findings, increasing the temporal code length enhances system performance. Furthermore, the acquired findings exhibit that the 2D-SFW code outperforms the 2D-DCS, 2D-MS, and 2D-ZCC/MD codes, increasing system capacity by 2.26, 3.76, and 1.5 times, respectively, and consuming less power reaches -16.3 dBm.

VII. REFERENCES

- [1] M. Rahmani, A. Cherifi, A. S. Karar, G. Naima Sabri, and B. S. Bouazza, 'Contribution of New Three-Dimensional Code Based on the VWZCC Code Extension in Eliminating Multiple Access Interference in Optical CDMA Networks', *Photonics*, vol. 9, no. 5, p. 310, May 2022, doi: 10.3390/photonics9050310.
- [2] M. Rahmani, A. Cherifi, G. N. Sabri, B. S. Bouazza, and A. Karar, 'Contribution of OFDM modulation to improve the performance of non-coherent OCDMA system based on a new variable weight zero cross correlation code', *Opt Quant Electron*, vol. 54, no. 9, p. 576, Sep. 2022, doi: 10.1007/s11082-022-03949-5.
- [3] M. Rahmani, G. N. Sabri, A. Cherifi, A. S. Karar, et H. Mrabet, 'Massive capacity of novel three-dimensional OCDMA-FSO system for next generation of high-data wireless networks', *Trans. Emerg. Telecommun. Technol.*, vol. 35, n^o 1, p. e4871, janv. 2024, doi: 10.1002/ett.4871.
- [4] A. Cherifi, H. Mrabet, B. S. Bouazza, and S. A. Aljunid, 'Performance enhancement of multiple access 3D-OCDMA networks using a pascal triangle codes', *Opt Quant Electron*, vol. 52, no. 2, p. 131, Feb. 2020, doi: 10.1007/s11082-020-2246-5.
- [5] A. Cherifi, N. Jellali, M. Najjar, S. A. Aljunid, and B. S. Bouazza, 'Development of a novel two-dimensional-SWZCC – Code for spectral/spatial optical CDMA system', *Optics & Laser Technology*, vol. 109, pp. 233–240, Jan. 2019, doi: 10.1016/j.optlastec.2018.07.078.
- [6] M. Alayed, A. Cherifi, A. F. Hamida, M. Rahmani, Y. Attalah, and B. S. Bouazza, 'Design improvement to reduce noise effect in CDMA multiple access optical systems based on new (2-D) code using spectral/spatial half-matrix technique', *Journal of Optical Communications*, vol. 0, no. 0, p. 000010151520200069, Sep. 2020, doi: 10.1515/joc-2020-0069.
- [7] H. Mrabet, A. Cherifi, T. Raddo, I. Dayoub, and S. Haxha, 'A Comparative Study of Asynchronous and Synchronous OCDMA Systems', *IEEE Systems Journal*, vol. 15, no. 3, pp. 3642–3653, Sep. 2021, doi: 10.1109/JSYST.2020.2991678.
- [8] M. N. Nurool, A. R. Arief, M. S. Anuar, S. A. Aljunid, N. Din Kerat, and S. Arif, 'Performance analysis of 2-D Extended-EDW Code for optical CDMA system', in *2014 2nd International Conference on Electronic Design (ICED)*, Penang, Malaysia: IEEE, Aug. 2014, pp. 287–292. doi: 10.1109/ICED.2014.7015815.
- [9] W. A. Imtiaz, H. Y. Ahmed, M. Zeghid, Y. Sharief, and M. Usman, 'Design and Implementation of Two-Dimensional Enhanced Multi-diagonal Code for High Cardinality OCDMA-PON', *Arab J Sci Eng*, vol. 44, no. 8, pp. 7067–7084, Aug. 2019, doi: 10.1007/s13369-019-03789-8.
- [10] M. Najjar, N. Jellali, and M. Ferchichi, 'Two-dimensional multi-service code for spectral/spatial optical CDMA system', *Opt Quant Electron*, vol. 49, no. 12, p. 397, Dec. 2017, doi: 10.1007/s11082-017-1234-x.
- [11] M. Najjar, N. Jellali, M. Ferchichi, and H. Rezig, 'Spectral/spatial optical CDMA code based on Diagonal Eigenvalue Unity', *Optical Fiber Technology*, vol. 38, pp. 61–69, Nov. 2017, doi: 10.1016/j.yofte.2017.08.003.
- [12] N. Jellali, M. Najjar, M. Ferchichi, and H. Rezig, 'Development of new two-dimensional spectral/spatial code based on dynamic cyclic shift code for OCDMA system', *Optical Fiber Technology*, vol. 36, pp. 26–32, Jul. 2017, doi: 10.1016/j.yofte.2017.02.002.
- [13] N. D. Kerat, S. Aljunid, C. Rashidi, and P. Ehkan, 'Performance of 2-D hybrid FCC-MDW code on OCDMA system with the presence of phase induced intensity noise', *ARPN J Eng Appl Sci*, vol. 11, no. 22, pp. 13203–8, 2016.
- [14] R. Matem, S. A. Aljunid, M. N. Junita, C. B. M. Rashidi, and I. S. Ahmed, 'Photodetector effects on the performance of 2D Spectral/Spatial code in OCDMA system', *Optik*, vol. 178, pp. 1051–1061, Feb. 2019, doi: 10.1016/j.ijleo.2018.10.068.
- [15] M. Rahmani, A. Cherifi, G. N. Sabri, M. I. Al-Rayif, I. Dayoub, et B. S. Bouazza, 'A novel 260 Gb/s 2D-OCDMA-FSO multiplexing system's performance evaluation for upcoming generations of high-speed wireless optical networks', *Opt. Quantum Electron.*, vol. 56, n^o 3, p. 449, mars 2024, doi: 10.1007/s11082-023-05947-7.
- [16] M. Alayed, A. Cherifi, A. Ferhat Hamida, and H. Mrabet, 'A fair comparison of SAC-OCDMA system configurations based on two dimensional cyclic shift code and spectral direct detection', *Telecommun Syst*, vol. 79, no. 2, pp. 193–212, Feb. 2022, doi: 10.1007/s11235-021-00840-8.
- [17] H. Mrabet, F. Bahloul, A. Karar, A. Cherifi, and A. Belghith, 'Nonlinear Effect and MAI Impact on SAC-OCDMA System Based on 2D Multi-Diagonal Code and Laser Array', *Applied Sciences*, vol. 11, no. 18, p. 8528, Sep. 2021, doi: 10.3390/app11188528.
- [18] M. Rahmani, A. Cherifi, G. Naima Sabri, M. I. Al-Rayif, I. Dayoub, et B. S. Bouazza, 'Performance investigation of 1.5 Tb/s optical hybrid 2D-OCDMA/OFDM system using direct spectral detection based on successive weight encoding algorithm', *Opt. Laser Technol.*, vol. 174, p. 110666, juill. 2024, doi: 10.1016/j.optlastec.2024.110666.
- [19] N. Jellali, F. Moez, and M. Najjar, 'Performance enhancement of OCDMA system based on 3D-Multi-Diagonal codes', in *2017 13th International Wireless Communications and Mobile Computing Conference (IWCMC)*, Valencia, Spain: IEEE, Jun. 2017, pp. 2105–2108. doi: 10.1109/IWCMC.2017.7986608.
- [20] H. Y. Ahmed, M. Zeghid, W. A. Imtiaz, T. Sharma, and A. Chehri, 'An efficient 2D encoding/decoding technique for optical communication system based on permutation vectors theory', *Multimedia Systems*, vol. 27, no. 4, pp. 691–707, Aug. 2021, doi: 10.1007/s00530-020-00711-3.
- [21] N. Jellali, M. Najjar, M. Ferchichi, and H. Rezig, 'Three-dimensional multi-diagonal codes for OCDMA system', *Optik*, vol. 145, pp. 428–435, Sep. 2017, doi: 10.1016/j.ijleo.2017.07.057.